

The effect of an anhydride curing agent, an accelerant, and non-ionic surfactants on the electrical resistivity of graphene/epoxy composites

Tzu Hsuan Chiang, Chun-Yu Liu, Ya-Chun Lin

Department of Energy Engineering, National United University, 2, Lienda, Nan-Shi Li, Miaoli, Taiwan 36063, Republic of China
Correspondence to: T.H. Chiang (E-mail: thchiang@nuu.edu.tw)

ABSTRACT: This study investigated different contents of an anhydride curing agent, an accelerant, and non-ionic surfactants on the electrical resistivity of cured graphene/epoxy composites. The anhydride curing agent was hexahydrophthalic anhydride (HHPA), the accelerant was 2-ethyl-4-methyl-1H-imidazole-1-propanenitrile (EMIP), and the non-ionic surfactants were Triton X surfactants with different numbers of polyethylene oxide (PEO) groups (m) that influence the electrical resistivity of cured graphene/epoxy composites. During the curing process, differential scanning calorimetry (DSC) was used to determine the effects of the extent of the crosslinking for different contents of the curing agent and how different enthalpy (ΔH) on the electrical resistivity of the cured graphene/epoxy composites was then generated. The cured graphene/epoxy composite—which consisted of a 1 : 0.85 weight ratio of epoxy resin and anhydride, a 0.5 wt % accelerant, and a 13 wt % graphene powder—had a low electrical resistivity of 11.68 Ω -cm and a thermal conductivity of 1.7 W/m·K. In addition, the cured composites contained a 1.0 wt % polyethylene glycol p-isooctylphenyl ether (X-100) surfactant, which effectively decreased their electrical resistivity. © 2015 Wiley Periodicals, Inc. *J. Appl. Polym. Sci.* 2015, 132, 41975

KEYWORDS: composites; crosslinking; graphene and fullerenes; nanotubes; surfactants

Received 31 October 2014; accepted 11 January 2015

DOI: 10.1002/app.41975

INTRODUCTION

Currently, many research investigations are being conducted on multi-functional composite adhesives because, in thermal management and electronic packaging applications, they provide thermal management, mechanical bonds, electrical connections, fewer processing steps, and lower curing temperatures than solder connection technology.¹ These polymer composites usually consist of organic materials, such as polymers or epoxy resins, and inorganic materials, such as carbon nanotubes (CNTs),² carbon nanofibers (CNF),³ graphene,⁴ carbon black,⁵ graphite,⁵ coke,⁵ and various metals, including copper,⁶ nickel,⁶ and silver¹ powders. One of the inorganic materials, graphene, has high electrical conductivity, excellent mechanical properties, and a better thermal conductivity than CNTs, CNFs, and other carbon filler-reinforced polymer composites.⁷ Recently, graphene has been extensively used in reinforced polymer composites as well as in several different fields, such as electronic devices,⁸ energy storage,⁹ sensors,¹⁰ electromagnetic interference (EMI) shielding,^{11,12} supercapacitors,^{13,14} secondary batteries,¹⁵ solar cells,¹⁶ and fuel cells.¹⁷ Graphene is also used to improve gas-barrier properties,¹⁸ lower electrical percolation thresholds,^{19,20} and utilized in biomedical applications,²¹ such as bio-sensing²² and bio-imaging.²³ Therefore, in this study, we used graphene

nanoplatelets to enhance the electrical and thermal conductivity of cured graphene/epoxy composites. This kind of graphene nanoplatelets is available on the market at a significantly lower price than the single-layer graphene. Some studies have investigated this kind of graphene nanoplatelets for electrical conductivity in composite, as shown in Table I, but apparently, our study has better electrical resistivity and thermal conductivity than the results of other studies because we used suitable types and content of a curing agent and accelerant as well as the X-100 surfactant to provide sufficient steric stabilization between particles, thereby helping the graphene particles homogeneously disperse in the cured composites.

In the curing process, both the curing agent (i.e., acids, anhydrides, and amines) and the accelerant (i.e., imidazole and tertiary amines) are important in the epoxy resin, subject to heating for processing the polymerization,³⁰ which determines the curing temperature and time, glass transition temperature, and mechanical and other physical properties. In fact, the epoxy/anhydride system is preferred in electronic applications³¹ because it provides thermostability and has good mechanical properties. Therefore, in this study, we used the epoxy/anhydride system as the organic materials in the graphene/epoxy composites. In the past few years, most research has focused on

Table I. Summary of Properties of Graphene Composite

| Graphene content (wt %) | Electrical resistivity (Ω -cm) | Thermal conductivity (W/m-K) | Reference |
|-------------------------|--|------------------------------|-----------|
| 3 | 100000 | - | 24 |
| 4 | 1587.3 | - | 25 |
| 5 | 9465900 | - | 26 |
| 6 | 11494.3 | 0.75 | This work |
| 10 | 3700 | - | 26 |
| | 1000 | - | 27 |
| | - | 0.5 | 28 |
| | 353.34 | 1.54 | This work |
| 13 | 11.69 | 1.7 | This work |
| 15 | 12048.2 | 0.73 | 29 |

investigating the kinetics of curing agents^{31–33} and accelerants.³⁴ To date, only one study (i.e., Lin *et al.*³⁵) has used curing agents, such as dicyandiamide (DICY), boron-amine complex, and imidazole derivatives, to formulate epoxy-based, isotropic conductive adhesives (ICAs) that affect electrical conductivity. The study also found that different contents of the anhydride curing agent and the accelerant in graphene/epoxy mixtures affected the cured composites' electrical conductivity and electrical resistivity. To date, no research has focused on an anhydride curing agent or accelerant. Thus, this study adopts this approach to determine the effect of an anhydride curing agent and an accelerant on the electrical resistivity of a cured graphene/epoxy composite.

The strong π - π interaction between graphene sheets makes it very difficult to disperse them homogeneously in some organic solvents and polymer matrices,²⁰ creating a challenge for them to form a continuous conductive network in a polymer matrix. As graphene is hydrophobic,³⁶ it readily aggregates in solvents and in polymer matrices. To overcome the graphene's aggregation problem, Guardia *et al.*³⁷ and Hasan *et al.*³⁶ studied the use of non-ionic surfactants to disperse graphene in water and N-methyl-2-pyrrolidone (NMP), respectively. The non-ionic surfactants tend to perform better than ionic surfactants in their ability to suspend graphene, as steric repulsion is more efficient than electrostatic repulsion in the stabilization of graphene sheets in water.³⁷

Therefore, in this study, we added non-ionic surfactants (i.e., Triton X surfactants) to the graphene/epoxy composite. The structure of Triton X surfactants consists of both a hydrophilic polyethylene oxide (PEO) group and hydrophobic hydrocarbon groups, such as the p-(1,1,3,3-tetramethylbutyl)-phenyl group. In previous research, which used paste, one of Triton X surfactants (i.e., X-100) was generally used to disperse CNT,^{38–40} carbon black,^{41,42} silica,⁴³ and poly(vinyl alcohol) fibers.⁴⁴ In the current study, a graphene/epoxy mixture was prepared using different types of Triton X surfactants in order to investigate how they affected the electrical resistivity of the cured graphene/epoxy composite. The study also investigated different contents of graphene powder in epoxy resin to determine the effect on thermal conductivity.

EXPERIMENTAL

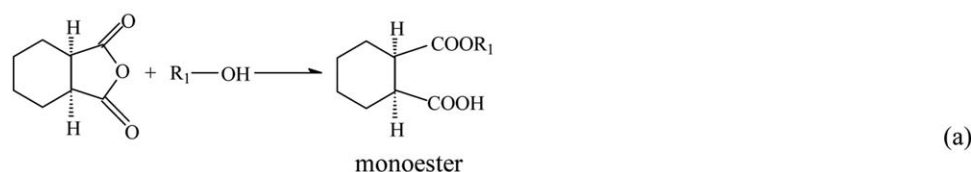
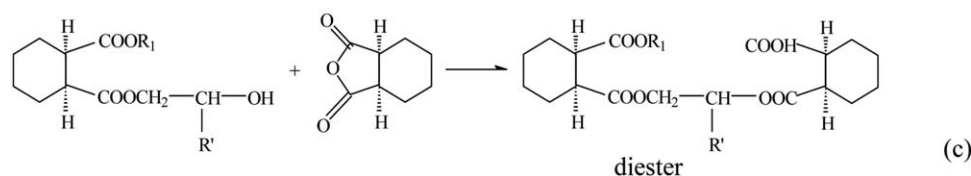
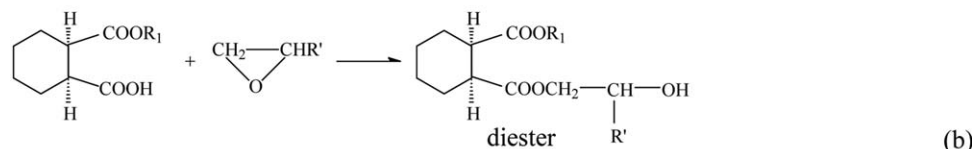
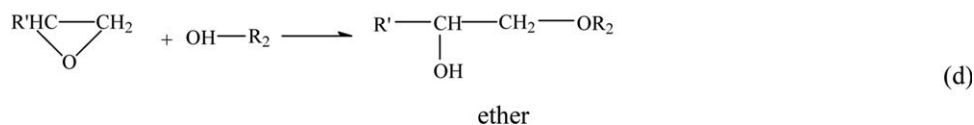
Preparation of Graphene/Epoxy Composites

One hundred grams of epoxy resin [as 3,4-epoxycyclohexylmethyl-3,4-epoxycyclohexanecarboxylate (UVR-6110) (supplied by Hubei Xinjing New Material, China)] were mixed with different curing agents—namely, hexahydrophthalic anhydride (HHPA, supplied by Sigma-Aldrich). The stoichiometry of epoxy resin and anhydrides adhered to 1 : 0.45, 1 : 0.65, 1 : 0.85, and 1 : 1 weight ratios. The accelerant used was 2-ethyl-4-methyl-1H-imidazole-1-propanenitrile (EMIP, supplied by Sigma-Aldrich), and the contents of the accelerant for the weight percentage of epoxy resin that was investigated were 0.2, 0.5, 0.8, and 1.0 wt %. The mixtures were mixed with different amounts of graphene powder (i.e., 6, 7, 10, and 13 wt %). The graphene powder was supplied by Enerage, Taiwan. The median diameter (D_{50}) was 17 μ m, the specific surface area was 20 cm²/g, and the average thickness of the sheet was <50 nm.

The graphene/epoxy mixtures were added into 1 wt % of different types of the Triton X surfactants consisting of polyoxyethylene-p-(1,1,3,3-tetramethylbutyl) phenyl ethers, which had different numbers of PEO groups, m , that represented different molecular distances, as shown in Table II. All of the surfactants were purchased from the Dow Chemical Company Co., Midland, Michigan.

Table II. Different Numbers of PEO Groups of Different Surfactants

| Chemical name of surfactants | Code name | m |
|---|-----------|-----|
| Polyethylene glycol 4-tert-octylphenyl ether | X-45 | 4.5 |
| Tert-octylphenoxy poly (ethoxyethanol) | X-114 | 7.5 |
| Polyethylene glycol p-isooctylphenyl ether | X-100 | 9.5 |
| Octylphenol ethoxylate | X-165 | 16 |
| 2-[4-(2,4,4-Trimethylpentan-2-yl)phenoxy] ethanol | X-305 | 30 |
| Polyethylene glycol tert-octylphenyl ether | X-405 | 35 |

Monoesterification**Esterification****Etherification**

Scheme 1. The curing reaction scheme for epoxy resin with HHPA.

The various mixtures were mixed via six millings in a milling process using a triple-roller mill (E-80, EXAKT, Germany) to form homogenous graphene/epoxy mixtures. All of the graphene/epoxy mixtures were then heated at 150°C for 30 min for curing.

Analysis of the Characteristics of Graphene/Epoxy Composites

Differential scanning calorimetry (DSC) measurements were performed in air using a Mettler Toledo DSC822 that had been calibrated by following standard procedures. The mixture was heated at 10°C/min from room temperature to approximately 300°C. The total heat of reaction (ΔH_T) was estimated by drawing a straight line that integrated the area under the line connecting the baseline of the exothermal peak. The residual enthalpy of the cured composite (ΔH_R) was obtained by heating the composite at 100°C/min from room temperature to 150°C and keeping the temperature constant for 30 min in air. After 30 min, the sample was cooled rapidly to 30°C in a DSC cell and then reheated at 10°C/min to 300°C. The conversion (α) was calculated using eq. (1)⁴⁵:

$$\alpha = \frac{\Delta H_T - \Delta H_R}{\Delta H_T} \quad (1)$$

The graphene/epoxy mixtures were printed on indium tin oxide (ITO) film using a 400-mesh, stainless-steel screen with an

emulsion (thickness of 12 μm) buildup mounted on a frame that measured 24.3 \times 29.7 cm. (The sheet resistance of the ITO film was $600 \pm 100 \Omega/\square$, and its thickness was $197 \pm 20 \mu\text{m}$. The product was purchased from EFUN Technology, Taiwan). The dimensions of the pattern were 1.5 \times 2 cm. The pattern was printed in only the forward direction using a squeegee that had a durometer hardness of 80. The pattern was used to measure the electrical resistivity of the cured graphene/epoxy composites using a four-point probe instrument manufactured by Everbeing International Corporation. These electrodes have a typical diameter of 0.4 mm and are separated by a distance of 1.5 mm. The electrical resistivity (ρ) was calculated using standardized testing protocol, SEMI MF84-0307,⁴⁶ as shown in eq. (2).

$$\rho = 4.532t \times (V/I) \quad (2)$$

where t is the thickness of the film, V is the voltage, and I is the DC electric current provided by a power supply (Tektronix, DMM40506-1/2 Digit Precision Multimeter).

The viscosities of the mixture were measured by a small sample adapter (25°C, 14 spindle and 10 rpm) of a viscometers (Model: HBDV-III U) from Brookfield. The microstructures and graphene dispersion of the cured graphene/epoxy

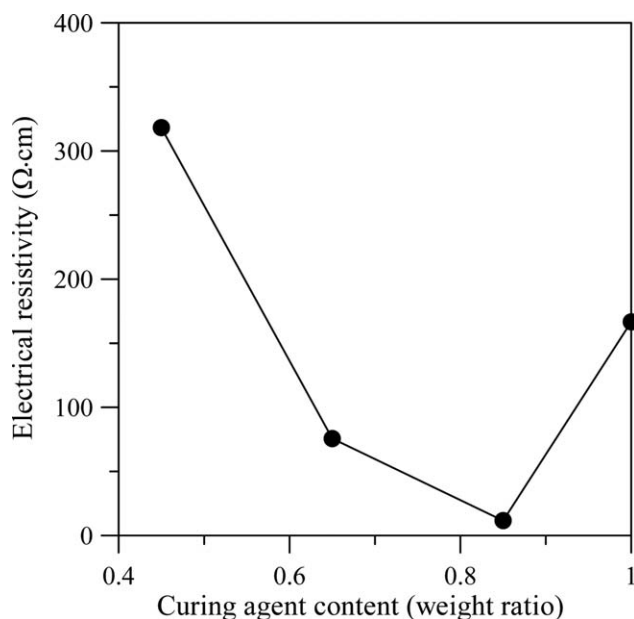


Figure 1. Electrical resistivity of the cured graphene/epoxy composites for different contents of the curing agent.

composites were observed using JEOL JED 2300 field emission scanning electronic microscopy (SEM), and transmission electron microscopy (TEM) images were obtained using a JEM 2010. The cured graphene/epoxy composites were prepared embedding polymer in an epoxy resin, and cutting ultra-thin sections were made at 50–70 nm using Leica Ultra Cut UCT Ultra microtome instrument equipped with a diamond knife for TEM analysis. The thermal conductivity coefficients of the cured graphene/epoxy composites were measured using a Hot Disk instrument (TPS 2500S, Sweden) that tested as standard according to ISO/DIS 22007-2.2, and the corresponding dimensions of the sample specimens were $30 \times 30 \times 0.8$ mm.

RESULTS AND DISCUSSION

Effect of Different Curing Agent Contents on Electrical Resistivity

The study used EMIP as a curing agent; its reaction mechanism for epoxy resin, shown in Scheme 1,^{47,48} has three main curing reactions—namely, monoesterification, esterification, and etherification.^{49,50} The anhydride ring had to be first opened by an active hydrogen, present as water, hydroxyls, or a Lewis base,⁵⁰ which generated an ester group and a carboxylic acid group, in order to bring about the formation of a monoester [Scheme 1(a)]. The newly formed carboxyl group then reacted quickly with the epoxy group and formed a diester and a new secondary hydroxyl group [Scheme 1(b)], thereby encouraging curing [Scheme 1(c)]. Ideally, the two reactions then proceed by alternating the addition of anhydride and epoxy until the sequence is terminated through the condensation of one terminal carboxylic acid and alcohol to an ester linkage. The etherification reaction in step Scheme 1(d) is epoxy homopolymerization, which is a competing reaction.

The electrical resistivity of the cured graphene/epoxy composites decreased as the curing agent increased from 1 : 0.45 to 1 : 0.85 weight ratio, as shown in Figure 1. Due to the degree of

crosslinking, the increase depends on the amount of the curing agent increase, forming a three-dimensional network of the adhesive increase. The network of the adhesive formed the graphene particles in the adhesive experiencing a compressive stress, which increased the particle in close contact¹ and improved adhesive conductivity. Therefore, the adhesives produced enthalpy (ΔH) that underwent a curing process according to DSC analysis, which can confirm the degree of crosslinking for adhesives, as shown in Figure 2 depicting that the ΔH values for different weight ratios of epoxy resin and curing agents (i.e., 1 : 0.45, 1 : 0.65, 1 : 0.85, and 1 : 1) were -302.1 , -444.9 , -974.2 , and -450.3 J/g, respectively. The results obtained about the extent of the crosslinking reaction for the different weight ratios of epoxy resin and curing agents produced values of ΔH as follows: 1 : 0.85 > 1 : 1 > 1 : 0.65 > 1 : 0.45. The increase in the crosslinking reactions of the mixtures was evidenced by the increase in the ΔH values as the curing agent content increased up to a 0.85 weight ratio in the graphene/epoxy mixtures. Therefore, the graphene/epoxy mixture containing a 0.85 weight ratio of the curing agent had the highest ΔH and the lowest electrical resistivity.

However, when the epoxy resin and curing agents mixed at the 1 : 1 weight ratio, the electrical resistivity of the cured composite increased to 166.7 Ω ·cm, which was higher than 1 : 0.85 (11.68 Ω ·cm). Due to an excessive amount of the curing agent (i.e., 1 : 1 weight ratio of epoxy resin and curing agent), the epoxy resin became diluted, which hindered the crosslinking reaction,^{32,51} causing the ΔH of mixture to be less than the ΔH of the mixture for 1 : 0.85, resulting in a higher electrical resistivity. In addition, an excessive amount of curing agent could cover the graphene's surface, resulting in increased resistance to tunneling.

Effect of Different Contents of the Accelerant for Electrical Resistivity

The EMIP as an accelerant in this study was applied to decrease the curing temperature of the mixtures, as a result of the

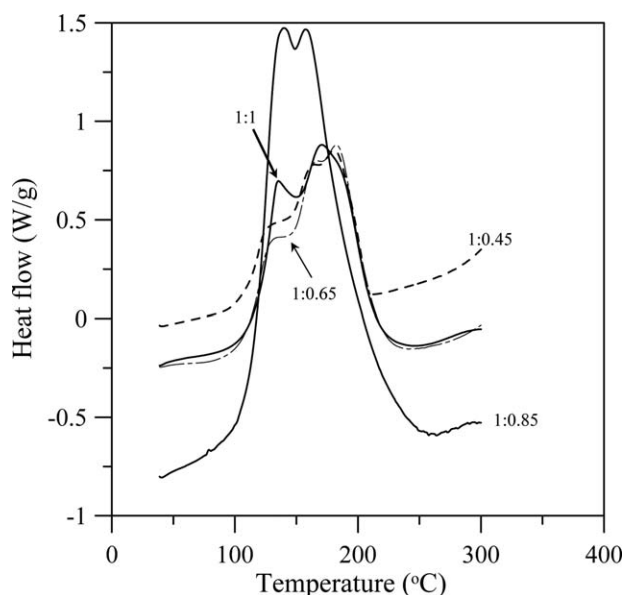
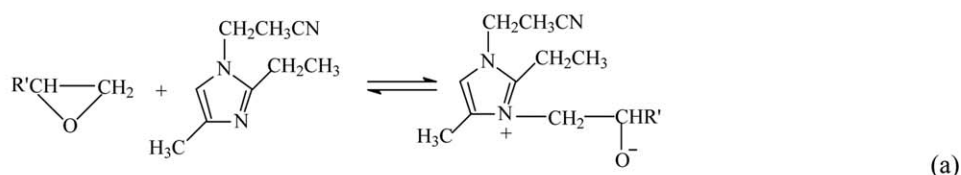
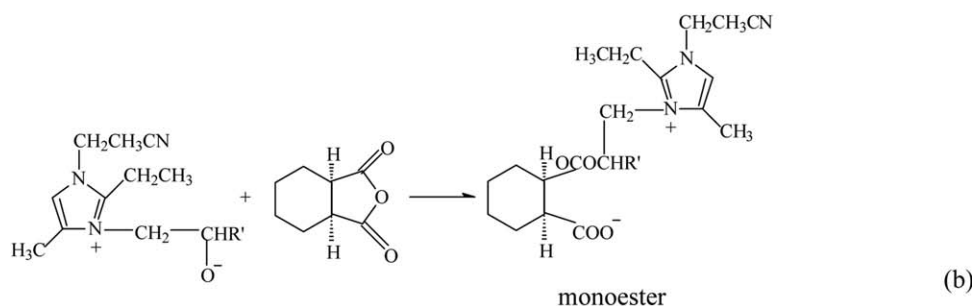
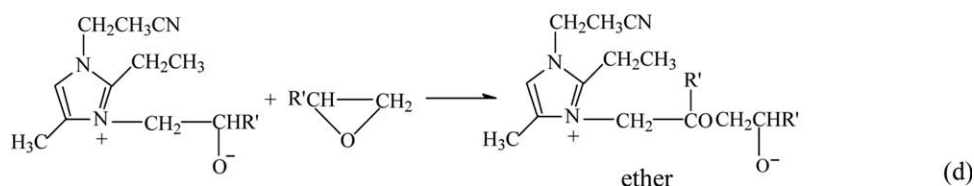
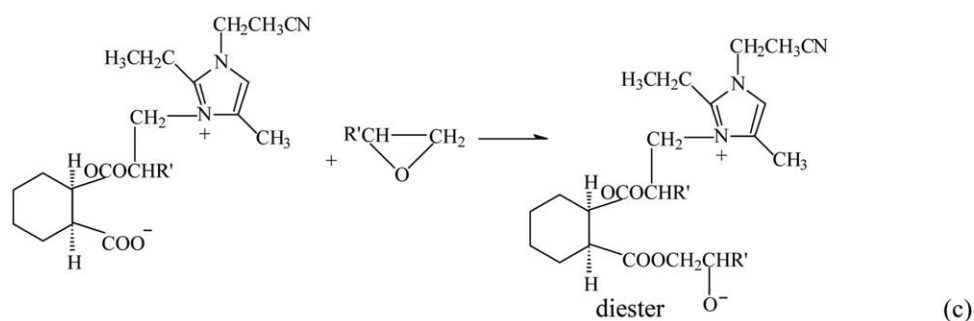


Figure 2. DSC curves of graphene/epoxy composites for different weight ratios of epoxy resin and curing agents during a dynamic cure.

Initiation**Esterification****Etherification**

Scheme 2. The curing reaction scheme for epoxy resin with HHPA and EMIP.

reaction mechanisms of the epoxy resin and anhydride curing agent (HHPA), as in Scheme 2,⁵² that have two principal curing reactions—namely, esterification and etherification^{52,53}—that were different from Scheme 1. First, the N atom of the accelerant (EMIP) attacked the epoxy group, producing an alkoxide ion as a zwitterion [Scheme 2(a)]. An alkoxide ion from the epoxy backbone reacted with the anhydride curing agent (HHPA) to produce a monoester [Scheme 2(b)] and a diester [Scheme 2(c)]. The reaction of the epoxy with an alkoxide ion, resulting in an ether linkage [Scheme 2(d)], was a competing reaction.

The different amounts of accelerant influenced the electrical resistivity of the cured graphene/epoxy composites, as shown in

Figure 3. The results demonstrated that the electrical resistivity (502.37 $\Omega\cdot\text{cm}$) of the cured graphene/epoxy composite with 0.2 wt % of accelerant was the largest and was higher than the cured composite without the accelerant (1.62 $\Omega\cdot\text{cm}$). Although the ΔH value (-723.29 J/g) of the graphene/epoxy mixture with 0.2 wt % of the accelerant was greater than without the accelerant ($\Delta H = -692.22$ J/g), as shown in Figure 4, and both mixtures were heated at 150°C for 30 min, an incomplete curing of some of the composite was demonstrated by its ΔH_R of -41.3 J/g and α of 0.94 (without an accelerant) and its ΔH_R of -16.2 J/g and α of 0.98 (with 0.2 wt % of accelerant), as shown in Figure 5. However, according to Schemes 1 and 2 of the curing mechanism, the products obtained as monoester molecular

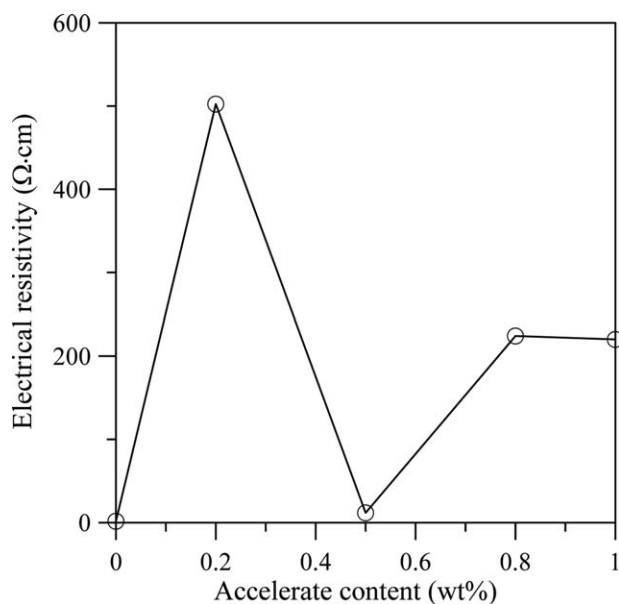


Figure 3. Electrical resistivity of the cured graphene/epoxy composites for different contents of accelerant.

weight [Scheme 2(b)] or diester molecular weight [Scheme 2(c)] for the graphene/epoxy mixture with 0.2 wt % of the accelerant subjected to heating at 150°C for 30 min (with incomplete curing, see Figure 5) were greater than products such as diester molecular weight for the graphene/epoxy composite without accelerant (with incomplete curing, see Figure 5). This situation was caused by the possible formation of a larger layer of organic matter that covered the surface of the graphene particle, which hindered the electrical transmission and resulted in increases in the electrical resistivity of the cured graphene/epoxy composites.

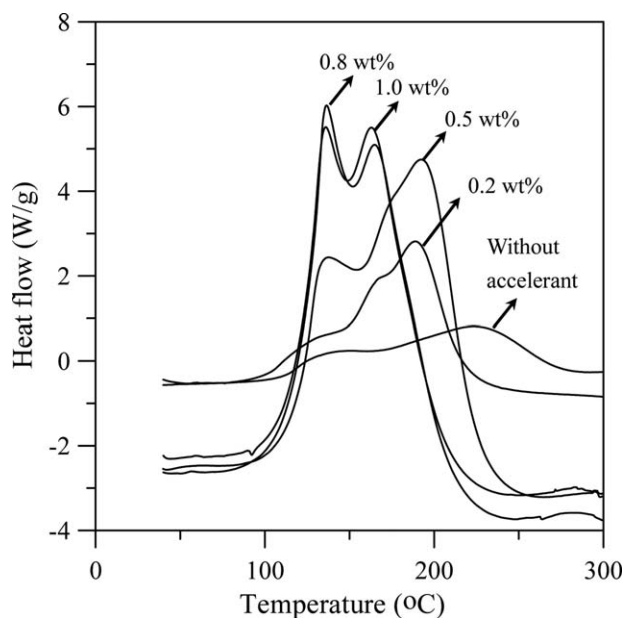


Figure 4. DSC curves of the graphene/epoxy composites for different contents of accelerant during a dynamic cure.

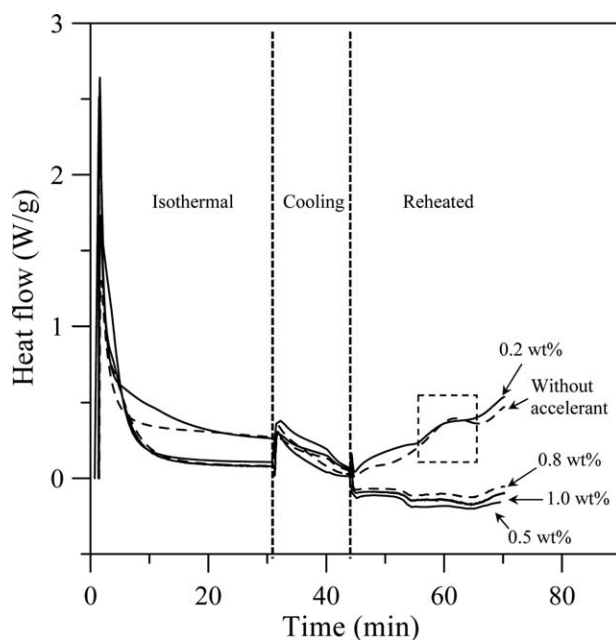


Figure 5. DSC curves of the graphene/epoxy composites that without accelerant and contained 0.2 wt % to 1.0 wt % of accelerant when they were subject to isothermal, cooling and reheating steps.

When the cured graphene/epoxy composite contained 0.5 wt % of accelerant, it had a low electrical resistivity of 11.68 $\Omega\cdot\text{cm}$, as shown in Figure 3, and its ΔH was -1268.13 J/g, as shown in Figure 4. The 0.5 wt % of accelerant helped the mixture cure completely ($\alpha = 1$) after subjecting it to heating at 150°C for 30 min, as shown in Figure 5. However, the electrical resistivity of the cured graphene/epoxy composite (11.68 $\Omega\cdot\text{cm}$) was higher than the cured graphene/epoxy composite without accelerant (1.62 $\Omega\cdot\text{cm}$). One reason for this could have been the large layer of organic matter that covered the surface of the graphene powder caused by the products as the diester molecular weight [Scheme 2(c)] or other molecular weight [Scheme 2(d)] of cured graphene/epoxy composite contained 0.5 wt % higher than the products of the diester molecular weight [Scheme 1(c)] or other molecular weight [Scheme 1(d)] of cured graphene/epoxy composite without accelerant.

In addition, when the proportion of the accelerant was increased to 0.8 and 1.0 wt % in the graphene/epoxy mixtures, the electrical resistivity of the cured composites increased to 224.23 and 220.08 $\Omega\cdot\text{cm}$ while their ΔH values increased to -3526.74 and -3262.57 J/g, respectively. The higher electrical resistivity occurred due to the excess diester [Scheme 2(c)] or ether [Scheme 2(d)] from 0.8 and 1.0 wt % of the accelerant in the cured composites, thereby hindering the electrical transmission.

Effect of Different Types of Surfactants for Electrical Resistivity

The surfactants have good dispersion for graphene powders, promoting have reduced viscosity of matrices, and lower electrical resistivity of composites. Figures 6 and 7 were show the electrical resistivities and viscosities of the various cured graphene/epoxy composites that contained 1.0 wt % of surfactants. The

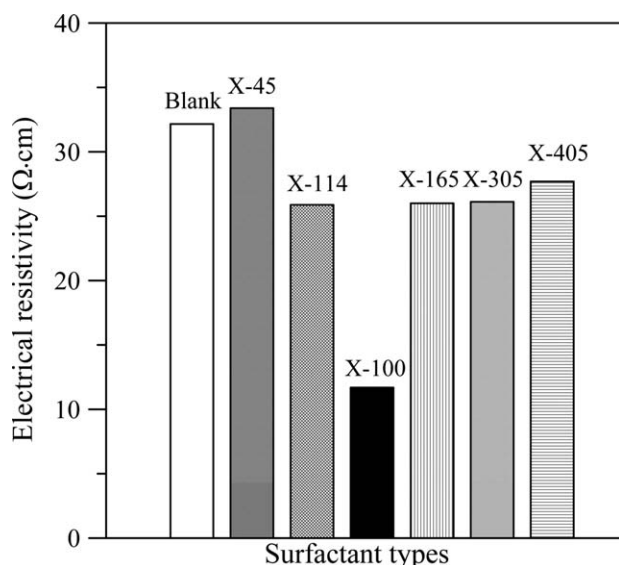


Figure 6. Electrical resistivity of cured graphene/epoxy composites for different surfactants.

electrical resistivity of the cured graphene/epoxy composite that contained X-45 was slightly higher than that of the graphene/epoxy mixture without the surfactant (blank). Because of the fewer number of PEO groups of X-45 ($m = 4.5$), indicating that the molecular distances of the PEO groups linked together are shorter, that it provides insufficient steric stabilization in the graphene/epoxy mixtures. Therefore, the viscosity of matrix contained X-45 was similar blank matrix when these matrices measured using a viscometers after 550 s, as shown in Figure 7. In addition, the molecular distance of X-114 ($m = 7.5$) was longer than of X-45 ($m = 4.5$), which has better steric stabilization in the graphene/epoxy mixtures, has a lower viscosity. Therefore, the electrical resistivity of the cured graphene/epoxy composite containing X-114 is lower than when it contains X-45.

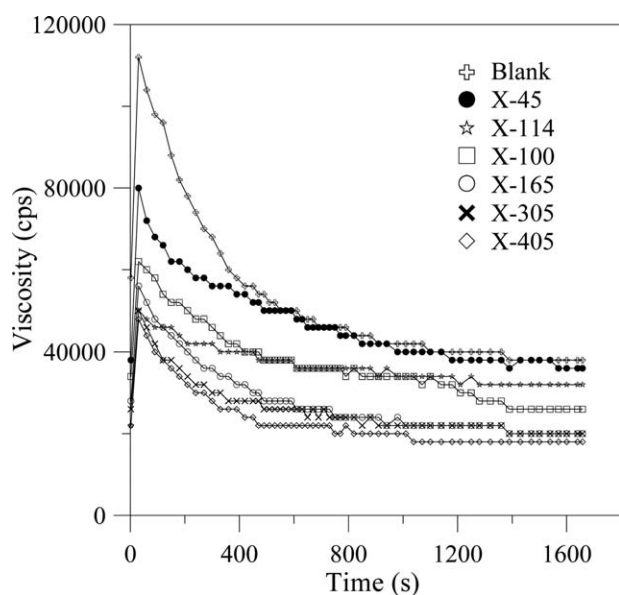


Figure 7. Viscosity of graphene/epoxy matrices for different surfactants.

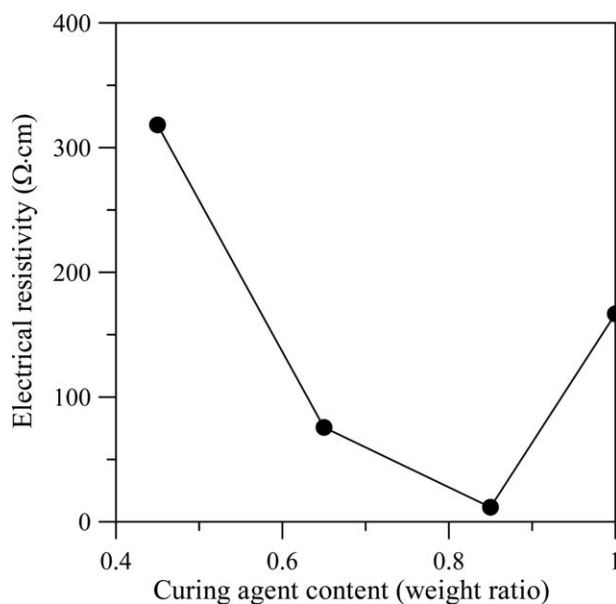


Figure 8. Electrical resistivity of the cured graphene/epoxy composites for different contents of X-100 surfactant.

The best improvement in the electrical conductivity of the cured graphene/epoxy composite occurred when X-100 was added. This result occurred because the X-100 had 9.5 PEO groups that were higher than X-45 and X-114, providing sufficient steric stabilization between the graphene particles to produce lower viscosity than X-45 and X-114. Guardia *et al.*³⁷ reported that non-ionic surfactants provided steric repulsion that was more efficient than electrostatic repulsion, thereby stabilizing the graphene powders in water by extending their ability to remain in suspension. However, when the PEO numbers of the surfactants exceeded 9.5, such as X-165 ($m = 16$), X-305 ($m = 30$), and X-405 ($m = 35$), this caused the electrical resistivity of cured composites to increase. Although these matrices have lower viscosity, but the molecular distances were much longer for X-165, X-305, and X-405, which hindered the electrical transmission and increased the electrical resistivity of cured graphene/epoxy composites.

Effect of Different Contents of the X-100 Surfactant for Electrical Resistivity

Figure 8 shows the electrical resistivity of the cured graphene/epoxy composites with different contents of X-100. The cured graphene/epoxy composite without any surfactant had an electrical resistivity of 35 Ω·cm. When the mixtures had 0.5 and 0.8 wt % of X-100, their electrical resistivity was larger than that of the cured composites without surfactants. This occurred because they provide insufficient steric stabilization in the graphene/epoxy mixtures, and the presence of some X-100 impeded the electrical transmission. When the 1.0 wt % of X-100 was added to the graphene/epoxy mixture, the cured composite had the lowest electrical resistivity at 11.68 Ω·cm. These results demonstrated that electrical resistivity of cured composites decreased according to the amount of X-100 following the sequence: 0.5 wt % > 0.8 wt % > 1.0 wt %.

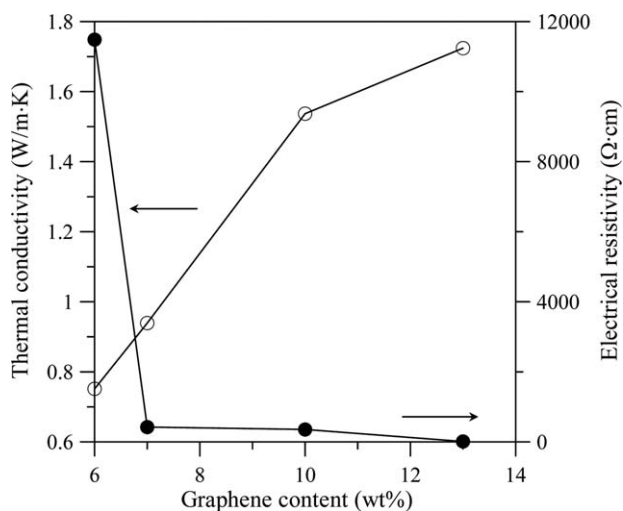


Figure 9. Thermal conductivity and electrical resistivity of cured graphene/epoxy composites for different contents of graphene powder.

However, when 1.2 and 1.5 wt % of X-100 were added to the graphene/epoxy mixtures, the electrical resistivity of the cured composites was larger than when 1.0 wt % of X-100 and no surfactant were added. Apparently, exceeding 1.0 wt % of X-100 in the graphene/epoxy mixture resulted in larger steric stabilization and caused larger distances between the graphene particles, which resulted in increased electrical resistivity.

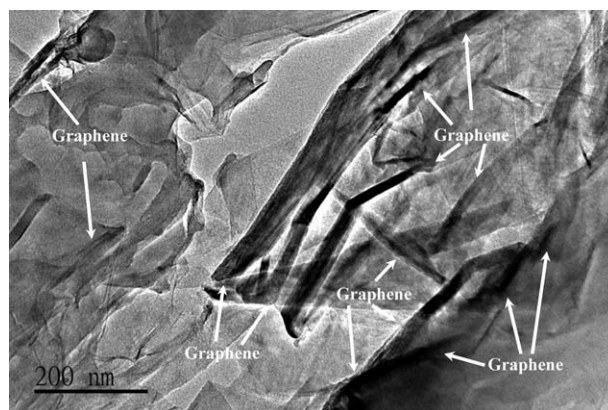


Figure 11. TEM images of the cured graphene/epoxy composite containing 13 wt % of graphene powder.

Effect of Graphene Content for Electrical Resistivity and Thermal Conductivity

Figure 9 shows the electrical resistivity and thermal conductivity of cured graphene/epoxy composites with different amounts of graphene powders. The results indicated that increasing the content of the graphene powder decreased the electrical resistivity and increased the thermal conductivity of the cured graphene/epoxy composites. Graphene powders were dispersed homogeneously in the mixture using different amounts, as shown in the SEM images of Figure 10. Therefore, when the cured graphene/epoxy composite contained 13 wt % of graphene powder, the

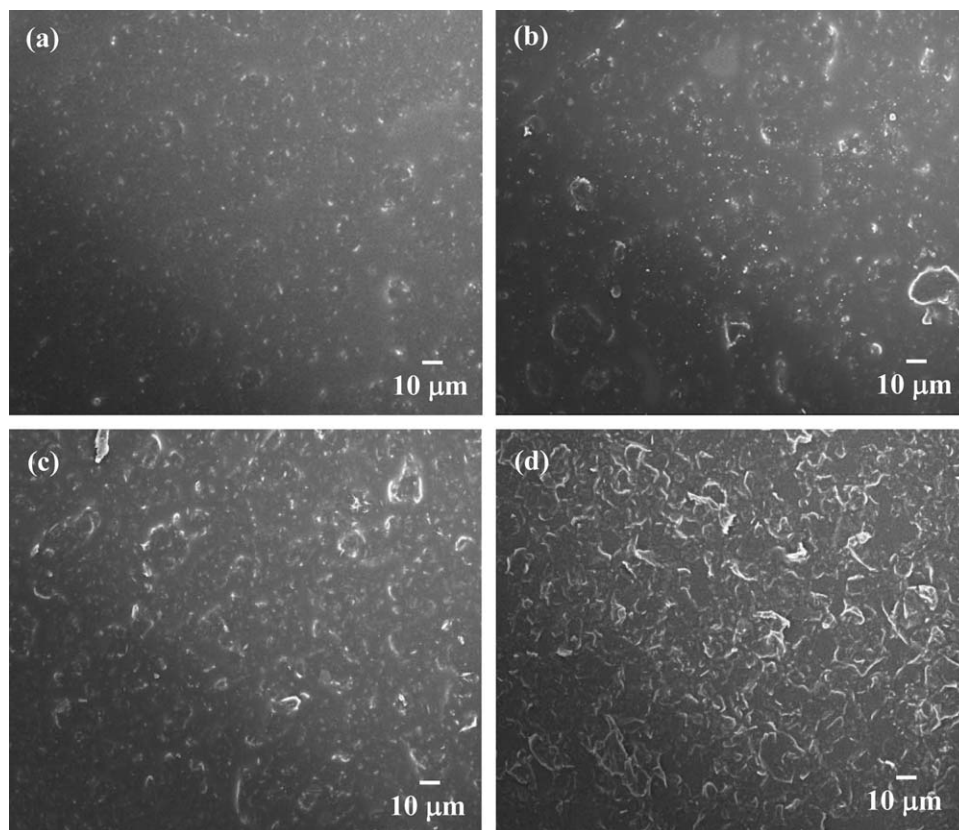


Figure 10. SEM images of cured graphene/epoxy composites for different contents of graphene powder: (a) 6 wt %; (b) 8 wt %; (c) 10 wt %; (d) 13 wt %.

between-particles content was more than other amounts, which generated the lowest electrical resistivity (11.69 Ω -cm) and the largest thermal conductivity (1.7 W/m-K). The TEM images of Figure 11 demonstrated that the 13 wt % of graphene powder was homogeneously dispersed, as was the between-particles content in the cured composites.

CONCLUSIONS

The results of this study indicate that inorganic material (i.e., graphene powder) and organic materials (i.e., curing agent, accelerant, and surfactants) affected the electrical resistivity of cured graphene/epoxy composites. The different contents of the curing agent affected the electrical resistivity depending on the degree of crosslinking. However, the excessive addition of the curing agent hindered the crosslinking reaction because the cured composite has higher electrical resistivity. In addition, the larger molecular weight of products for cured composites formed a large layer of organic matter that covered the surface of the graphene powder, causing higher electrical resistivity of cured composites. Thus, the 1 : 0.85 weight ratio of the epoxy resin and curing agent and the use of the 0.5 wt % accelerant resulted in low electrical resistivity (11.68 Ω -cm) for the cured graphene/epoxy composites.

Different numbers of PEO groups for the Triton X surfactants provided different steric stabilization between the graphene particles, which affected the electrical resistivity of the cured graphene/epoxy composites. The study demonstrated that graphene/epoxy composites containing 1.0 wt % of X-100 surfactant had sufficient steric stabilization between the graphene particles that further reduced the electrical resistivity more than other surfactants and other content ratios. In addition, the cured graphene/epoxy composite containing 13 wt % of graphene powder had the lowest electrical resistivity (11.68 Ω -cm) and the largest thermal conductivity (1.7 W/m-K).

ACKNOWLEDGMENTS

The authors thank the TechMax Technical of Taiwan for providing analyst of thermal conductivity of t graphene/epoxy composite.

REFERENCES

- Kim, H. K.; Shi, F. G. *Microelectron. J.* **2001**, *32*, 315.
- Szentes, A.; Varga, Cs.; Horváth, G.; Bartha, L.; Kónya, Z.; Haspel, H.; Szél, J.; Kukovecz, Á. *Exp. Polym. Lett.* **2012**, *6*, 494.
- Feng, L.; Xie, N.; Zhong, J. *Materials* **2014**, *7*, 3919.
- Wang, Y.; Yu, J.; Dai, W.; Song, Y.; Wang, D.; Zeng, L.; Jiang, N. *Polym. Compos.* **2014**, DOI: 10.1002/pc.22972.
- King, J. A.; Miller, M. G.; Barton, R. L.; Keith, J. M.; Hauser, R. A.; Peterson, K. R.; Sutter, L. L. *J. Appl. Polym. Sci.* **2006**, *99*, 1552.
- Mamunya, Y. P.; Davydenko, V. V.; Pissis, P.; Lebedev, E. V. *Eur. Polym. J.* **2002**, *38*, 1887.
- Zhao, C.; Zhang, G.; Zhao, L. *Molecules* **2012**, *17*, 8587.
- Eda, G.; Chhowalla, M. *Nano Lett.* **2009**, *9*, 814.
- Radich, J. G.; McGinn, P. J.; Kamat, P. V. *Interface* **2011**, *20*, 63.
- Yang, T.; Zhang, H.; Wang, Y.; Li, X.; Wang, K.; Wei, J.; Wu, D.; Li, Z.; Zhu, H. *Nano Res.* **2014**, *7*, 869.
- Wang, S.; Tambraparni, M.; Qiu, J.; Tipton, J.; Dean, D. *Macromolecules* **2009**, *42*, 5251.
- Eswaraiyah, V.; Sankaranarayanan, V.; Ramaprabhu, S. *Macromol. Mater. Eng.* **2011**, *296*, 894.
- Sun, Y.; Shi, G. *J. Polym. Sci. Part. B-Polym. Phys.* **2013**, *51*, 231.
- Stoller, M. D.; Park, S.; Zhu, Y.; An, J.; Ruoff, R. S. *Nano Lett.* **2008**, *8*, 3498.
- Yoo, E.; Kim, J.; Hosono, E.; Zhou, H. S.; Kudo, T.; Honma, I. *Nano Lett.* **2008**, *8*, 2277.
- Hong, W.; Xu, Y.; Lu, G.; Li, C.; Shi, G. *Electrochem. Commun.* **2008**, *10*, 1555.
- Kou, R.; Shao, Y.; Wang, D.; Engelhard, M. H.; Kwak, J. H.; Wang, J.; Viswanathan, V. V.; Wang, C.; Lin, Y.; Wang, Y.; Aksay, I. A.; Liu, J. *Electrochem. Commun.* **2009**, *11*, 954.
- Yoo, B. M.; Shin, H. J.; Yoon, H. W.; Park, H. B. *J. Appl. Polym. Sci.* **2014**, *131*, 39628.
- He, L.; Tjong, S. C. *Nanoscale Res. Lett.* **2013**, *8*, 132.
- Zhou, T. N.; Qi, X. D.; Fu, Q. *Exp. Polym. Lett.* **2013**, *7*, 747.
- Shen, H.; Zhang, L.; Liu, M.; Zhang, Z. *Theranostics* **2012**, *2*, 283.
- Wang, Y.; Shao, Y. Y.; Matson, D. W.; Li, J.; Lin, Y. *ACS Nano* **2010**, *4*, 1790.
- Sun, X. M.; Liu, Z.; Welsher, K.; Robinson, J. T.; Goodwin, A.; Zaric, S.; Dai, H. *Nano Res.* **2008**, *1*, 203.
- Monti, M.; Rallini, M.; Puglia, D.; Peponi, L.; Torre, L.; Kenny, J. M. *Compos. Pt. A-Appl. Sci. Manuf.* **2013**, *46*, 166.
- Ding, J. N.; Fan, Y.; Zhao, C. X.; Liu, Y. B.; Yu, C. T.; Yuan, N. Y. *J. Compos. Mater.* **2012**, *46*, 747.
- Sedaghat, A.; Ram, M. K.; Zayed, A.; Kamal, R.; Shanahan, N. *Open J. Compos. Mater.* **2014**, *4*, 12.
- An, J. E.; Jeong, Y. G. *Eur. Polym. J.* **2013**, *49*, 1322.
- Kim, S. Y.; Noh, Y. J.; Yu, J. *Compos. Pt. A-Appl. Sci. Manuf.* **2015**, *69*, 219.
- Tien, D. H.; Park, J.; Han, S. A.; Ahmad, M.; Seo, Y. *J. Korean Phys. Soc.* **2011**, *59*, 2760.
- Gan, J.; Rosenthal, C.; Eckert, M. M.; Kainz, B.; Trottier, E. C. U.S. Pat. 20,100,317,768, **2010**.
- Naito, C.; Todd, M. *Microelectron. Reliab.* **2002**, *42*, 119.
- Mauri, A. N.; Riccardi, C. C. *J. Appl. Polym. Sci.* **2002**, *85*, 2342.
- Guerrero, P.; De la Caba, K.; Valea, A.; Corcuera, M. A.; Mondragon, I. *Polymer* **1996**, *37*, 2195.
- Chun, I. S.; Shim, M. J.; Kim, S. W. *J. Ind. Eng. Chem.* **1999**, *2*, 40.
- Lin, X.; Li, Q.; Zhang, J. Electronic Materials and Packaging, 2006 (EMAP 2006), International Conference on, Kowloon, Hong Kong, December 11–14, 2006.
- Hasan, T.; Scardaci, V.; Tan, P. H.; Bonaccorso, F.; Rozhin, A. G.; Sun, Z.; Ferrari, A. C. In Molecular- and Nano-Tubes;

- Hayden, O.; Nielsch, K., Eds.; Springer: New York, **2011**, Chapter 9, p 279.
37. Guardia, L.; Fernández-Merino, M. J.; Paredes, J. I.; Solís-Fernández, P.; Villar-Rodil, S.; Martínez-Alonso, A.; Tascón, J. M. D. *Carbon* **2011**, *49*, 1653.
38. Bai, Y.; Lin, D.; Wu, F.; Wang, Z.; Xing, B. *Chemosphere* **2010**, *79*, 362.
39. Li, J.; Zhang, Q.; Li, H.; Chan-Park, M. B. *Nanotechnology* **2006**, *17*, 668.
40. Randhawa, P.; Park, J. S.; Sharma, S.; Kumar, P.; Shin, M. S.; Sekhon, S. *J. Nanoelectron. Optoelectron.* **2012**, *7*, 1.
41. Furuya, N.; Mineo, N. *J. New Mat. Electrochem. Syst.* **2007**, *10*, 205.
42. Zhang, Z.; Qu, C.; Zheng, T.; Lai, Y.; Li, J. *Int. J. Electrochem. Sci.* **2013**, *8*, 6722.
43. Alexeev, V. L.; Ilekci, P.; Persello, J.; Lambard, J.; Gulik, T.; Cabane, B. *Langmuir* **1996**, *12*, 2392.
44. Araújo, E. S.; Nascimento, M. L. F.; de Oliveira, H. P. *Fibres Text East Eur.* **2013**, *4*, 39.
45. Montserrat, S.; Flaque, C.; Page, P.; Malek, J. *J. Appl. Polym. Sci.* **1995**, *56*, 1413.
46. SEMI MF84-0307—Test method for measuring resistivity of silicon wafers with an in-line four-point probe, 2006.
47. Fisch, W.; Hofmann, W. *J. Polym. Sci.* **1954**, *121*, 497.
48. Fisch, W.; Hofmann, W.; Kaskikallio, J. *J. Appl. Chem.* **1956**, *6*, 429.
49. Weiss, H. K. *Ind. Eng. Chem.* **1957**, *49*, 1089.
50. Grimsley, B. W.; Hubert, P.; Song, X.; Cano, R. J.; Loos, A. C.; Pipes, R. B. *Sample J.* **2002**, *38*, 8.
51. Zhao, X.; Zhang, Q.; Chen, D. *Macromolecules* **2010**, *43*, 2357.
52. Park, W. H.; Lee, J. K.; Kwon, K. *J. Polym. J.* **1996**, *28*, 407.
53. Farbas, A.; Strohm, P. F. *J. Appl. Polym. Sci.* **1968**, *12*, 159.